

# The Double Role of Comonomers on the Crystallization Behavior of Isotactic Polypropylene: Propylene–Hexene Copolymers

Claudio De Rosa,<sup>\*,†</sup> Finizia Auriemma,<sup>†</sup> Odda Ruiz de Ballesteros,<sup>†</sup> Dario De Luca,<sup>†</sup> and Luigi Resconi<sup>‡</sup>

Dipartimento di Chimica “Paolo Corradini”, Università di Napoli “Federico II”, Complesso Monte S. Angelo, Via Cintia, I-80126 Napoli, Italy, and Basell Polyolefins, Centro Ricerche G. Natta, P. le G. Donegani 12, I-44100 Ferrara, Italy

Received August 4, 2007; Revised Manuscript Received January 8, 2008

**ABSTRACT:** A study of the crystallization behavior of isotactic propylene–hexene copolymers prepared with metallocene catalysts is reported. These copolymers crystallize from the melt as mixtures of  $\alpha$  and  $\gamma$  forms of isotactic polypropylene (iPP). The amount of  $\gamma$  form first increases very rapidly with increasing hexene concentration, up to 2–3 mol %, and then rapidly decreases for hexene concentrations higher than 4–5 mol %, and samples with hexene contents higher than 10 mol % (and lower than 15–16 mol %) crystallize from the melt exclusively in the  $\alpha$  form. This is due to the fact that at high concentrations hexene units enter to high extents into crystals of  $\alpha$  form, driven by density increase, favoring crystallization of the  $\alpha$  form instead of that of the  $\gamma$  form. These data have confirmed that the crystallization of  $\gamma$  form of iPP is not only related to the value of the average length of the regular propylene sequences but also related to the different degrees of inclusion of stereodefects and constitutional defects in the crystals of  $\alpha$  and  $\gamma$  forms.

## Introduction

The structure of isotactic propylene–hexene random copolymers (iPPHe), prepared with metallocene catalysts, has been described in recent papers.<sup>1–4</sup> It has been observed that iPPHe copolymers crystallize in the  $\alpha$  form of isotactic polypropylene (iPP) for low concentrations of hexene comonomeric units, up to nearly 10 mol %, and in the new trigonal form for hexene contents higher than 10 mol %.<sup>1–4</sup> Hexene units are partially included in both crystals of  $\alpha$  form and of the trigonal form.<sup>1,2</sup> The crystallization of the new trigonal form at high hexene concentrations allows incorporation of amounts of hexene units higher than in crystals of  $\alpha$  form.<sup>1–4</sup> The inclusion of hexene units in the crystals induces a suitable increase of density that allows crystallization of 3-fold helical chains in the trigonal form, where the helical symmetry of the chains is maintained in the crystal lattice (space group  $R\bar{3}c$ ),<sup>1,2</sup> giving a structure similar to that of form I of isotactic polybutene (iPB).<sup>5</sup> This form has never been observed for iPP homopolymer because, in the absence of bulky side groups, it would have a too low density.<sup>1,2</sup>

The phase transformation of the  $\alpha$  form into the trigonal form with increasing hexene concentration represents a clear example of the influence of the presence of defects on the polymorphic behavior of iPP. A study of the effect of the presence of ethylene and butene comonomers on the crystallization behavior of iPP, in particular the crystallization of  $\alpha$  and  $\gamma$  forms, has been recently reported.<sup>6</sup> It has been found that the crystallization of  $\gamma$  form is favored by the presence of ethylene, and samples of propylene–ethylene copolymers with ethylene concentration higher than 10 mol % crystallize from the melt completely in the  $\gamma$  form. For propylene–butene copolymers, instead, the amount of  $\gamma$  form decreases for butene concentrations higher than 10–14 mol %, and samples with butene contents higher

than 25–30 mol % crystallize from the melt exclusively into  $\alpha$  form because of inclusion of butene units in crystals of  $\alpha$  form.<sup>6</sup> These data indicated that the crystallization of  $\gamma$  form of iPP is not only related to the value of the average length of the regular propylene sequences but also related to the different degrees of inclusion of defects in the crystals of  $\alpha$  and  $\gamma$  forms of iPP.

In this paper we report a study of the effect of the presence of hexene units on the crystallization of  $\alpha$  and  $\gamma$  forms of iPP. Since the inclusion of hexene units in the crystals of  $\alpha$  form of iPP has been demonstrated in our recent papers,<sup>1,2</sup> the study of the crystallization behavior of iPPHe copolymers affords the opportunity to analyze the double role played by defects on the crystallization of iPP, that is, the interruption of regular propylene sequences and the inclusion of defects in crystals of  $\alpha$  and  $\gamma$  forms.

## Experimental Part

Samples of iPPHe copolymers have been prepared in liquid monomers or hexane solutions at temperatures between 50 and 70 °C with the  $C_2$ -symmetric metallocene catalysts shown in Chart 1, activated with methylalumoxane (MAO). All samples are listed in Table 1. The number  $N$  in the symbol iPPHe $N$  indicates the hexene concentration in mol % in the copolymer.

The highly isoselective  $C_2$ -symmetric metallocenes **A**<sup>7,8</sup> and **B**<sup>9</sup> produce high molecular mass and highly stereoregular iPP homopolymer and iPPHe copolymers containing very small concentrations of stereoerrors (about 0.2 mol % of  $rr$  triad defects) and regiodefects due to secondary 2,1-erythro (2,1e) insertions of propylene units (nearly 0.8 mol % in the homopolymer sample iPPA; see Table 1).<sup>7–9</sup> Regioinverted hexene units could not be identified by <sup>13</sup>C NMR. The microstructural data of all samples have been obtained from <sup>13</sup>C NMR analysis.<sup>10</sup>

The mass average molecular masses were evaluated from size exclusion chromatography (SEC). The SEC curves of all samples show narrow molecular weight distributions, with  $M_w/M_n \approx 2$ , typical of single-center metallocene catalysts. Narrow molecular weight distributions and  $r_1r_2$  values, evaluated according to ref 11, close to 1 indicate that copolymers have a random distribution of comonomers and homogeneous intermolecular composition.

\* To whom correspondence should be addressed: Tel ++39 081 674346; Fax ++39 081 674090; e-mail claudio.derosa@unina.it.

<sup>†</sup> Università di Napoli “Federico II”.

<sup>‡</sup> Basell Polyolefins.

Chart 1. Structures of Metallocenes Used in This Study

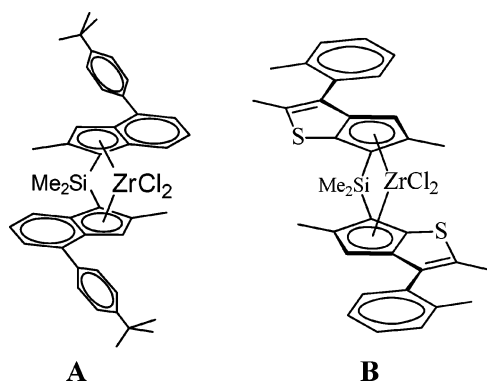


**Table 1. Compositions (mol % Hexene), Weight-Average Molecular Masses ( $\bar{M}_w$ ), Polydispersities ( $\bar{M}_w/\bar{M}_n$ ), Melting Temperatures of As-Polymerized Samples ( $T_m$ ), Contents of Stereoerrors ( $rr$ ), Concentrations of Secondary 2,1-Erythro Units (2,1e), and Total Concentration of Defects ( $\epsilon$ ) of Homopolymer Sample iPPA and Propylene–Hexene Copolymers Prepared with the MAO Activated Metallocenes of Chart 1**

sample	mol % hexene	$\bar{M}_w$	$\bar{M}_w/\bar{M}_n$	$T_m$ (°C) <sup>a</sup>	[ $rr$ ] (%) <sup>b</sup>	[2,1e] (%) <sup>c</sup>	$\epsilon$ (%) <sup>d</sup>
iPPA	0	237 500	2.2	151	0.2	0.8	1.0
iPPHe1.2	1.2	699 600	2.3	143	0.2	0.1	1.5
iPPHe2.0	2.0	122 000	2.4	129	0.2	0.2	2.4
iPPHe2.5	2.5	430 800	2.0	127	0.2	0.2	2.9
iPPHe3.2	3.2	152 000	2.0	124	0.2	0.2	3.6
iPPHe3.7	3.7	333 200	2.0	120	0.2	0.2	4.1
iPPHe4.2	4.2	291 700	2.0	115	0.2	0.2	4.6
iPPHe6.8	6.8	239 500	2.2	99	0.2	0.1	7.1
iPPHe9.0	9.0	209 800	2.0	93	0.2	0.1	9.3
iPPHe11.2	11.2	266 300	1.9	65	0.2	0.1	11.5
iPPHe18 <sup>e</sup>	18.0	217 400	1.9	49	3.5	0	21.5
iPPHe26	26.0	184 500	2.0	50	0.2	0.1	26.3

<sup>a</sup> Melting temperatures of as-prepared samples from DSC scans at heating rate of 10 °C/min. <sup>b</sup> [ $rr$ ] is the percentage of primary stereoerrors over all monomer units, [ $rr$ ] = [ $mrrm$ ] + [ $mrrr$ ]. It is not determinable for iPPHe samples and is assumed to be the same as that found in the corresponding homopolymer iPPA. <sup>c</sup> Secondary insertions 2,1e are only of the erythro type, and their amount is normalized over all monomer units. <sup>d</sup>  $\epsilon$  = [ $rr$ ] + [2,1e] + [hexene]. <sup>e</sup> Sample prepared with a  $C_1$ -symmetric catalyst (metallocene **D** of ref 6).

The melting temperatures were obtained with a differential scanning calorimeter (DSC) Perkin-Elmer DSC-7 performing scans in a flowing  $N_2$  atmosphere and heating rate of 10 °C/min. X-ray powder diffraction profiles were obtained with Ni filtered Cu K $\alpha$  radiation with an automatic Philips diffractometer.

The various iPPHe copolymer samples were isothermally crystallized from the melt at different temperatures. Powder samples were melted at 200 °C and kept for 5 min at this temperature in a  $N_2$  atmosphere; they were then rapidly cooled to the crystallization temperature,  $T_c$ , and kept at this temperature, still in a  $N_2$  atmosphere, for a time long enough to allow complete crystallization at  $T_c$ . The samples were then rapidly cooled to room temperature and analyzed by X-ray diffraction.

The relative amount of crystals in the  $\gamma$  form present in our samples was determined from the X-ray diffraction profiles, by measuring the ratio between the intensities of the (117) $_{\gamma}$  reflection at  $2\theta = 20.1^\circ$ , typical of the  $\gamma$  form, and the (130) $_{\alpha}$  reflection at  $2\theta = 18.6^\circ$ , typical of the  $\alpha$  form:  $f_{\gamma} = I(117)_{\gamma}/[I(130)_{\alpha} + I(117)_{\gamma}]$ .

## Results and Discussion

The X-ray powder diffraction profiles of some samples of iPPHe copolymers isothermally crystallized from the melt at different crystallization temperatures are reported in Figure 1. The diffraction profiles of the samples as-polymerized and aged at room temperature for long time are also reported in Figure 1

(profiles a) for comparison. While as-polymerized and aged samples are crystallized in the  $\alpha$  form, all samples crystallize from the melt as mixtures of  $\alpha$  and  $\gamma$  forms, as indicated by the presence in the diffraction profiles of Figure 1 of both (130) $_{\alpha}$  and (117) $_{\gamma}$  reflections at  $2\theta \approx 18.6^\circ$  and  $20^\circ$  of  $\alpha$  and  $\gamma$  forms, respectively. For each sample, the fraction of  $\gamma$  form with respect to the  $\alpha$  form increases with increasing crystallization temperature, as indicated by the increase of the intensity of the (117) $_{\gamma}$  reflection of the  $\gamma$  form with increasing crystallization temperature. For hexene contents higher than 9–10 mol % the as-polymerized and aged samples contain small amount of crystals of the trigonal form, as indicated by the presence of the (110) $_T$  reflection at  $2\theta = 10^\circ$  of the trigonal form in the diffraction profile a of Figure 1E, but the samples always crystallize from the melt only in the  $\alpha$  form (Figure 1E).

Contrary to all data reported in the literature that show increase of the amount of  $\gamma$  form crystallized from the melt with increasing concentration of microstructural defects, that is *stereo*- and *regio*-irregularities<sup>12–17</sup> and comonomeric units,<sup>18–21</sup> for iPPHe copolymers the amount of  $\gamma$  form in melt-crystallized samples increases with increasing hexene concentration only up to 2–3 mol % (Figure 1A,B). A clear decrease of concentration of  $\gamma$  form is observed for hexene concentrations higher than 3–4 mol % (compare parts B–D of Figure 1) and samples with hexene contents higher than 10 mol % (and lower than 15–16 mol %) crystallize from the melt exclusively in the  $\alpha$  form at any crystallization temperature (Figure 1E). Samples with hexene concentration higher than 15–16 mol % do not crystallize from the melt, and amorphous samples crystallize in the trigonal form by aging at room temperature.<sup>2</sup> This behavior is different from that of samples of propylene–ethylene copolymers that crystallize from the melt completely in the  $\gamma$  form at any crystallization temperature when the ethylene concentration is higher than 10 mol %.<sup>6,19b</sup> The behavior of iPPHe copolymers is instead similar to that of propylene–butene copolymers, for which the amount of  $\gamma$  form in melt-crystallized samples decreases for butene concentrations higher than 14–15 mol % and samples with butene contents higher than 25–30 mol % crystallize from the melt exclusively into  $\alpha$  form at any crystallization temperature.<sup>6</sup> The only difference is the formation of the trigonal form in iPPHe copolymers for hexene contents higher than 15–16 mol % and continuation of the  $\alpha$  form in propylene–butene copolymers at high butene concentration.

The values of relative amount of the  $\gamma$  form with respect to the  $\alpha$  form,  $f_{\gamma}$ , in the various samples of iPPHe copolymers, are reported in Figure 2 as a function of the crystallization temperature. Data of amount of  $\gamma$  form for melt-crystallized samples of the homopolymer iPPA, prepared with the same catalyst **A**, already reported in the literature,<sup>15a</sup> are also reported in Figure 2 for comparison.

As already observed in the literature for stereoirregular samples of iPP homopolymer<sup>12–17</sup> and iPP-based copolymers,<sup>6,18–21</sup> for each sample the content of  $\gamma$  form increases with increasing crystallization temperature and a maximum amount of  $\gamma$  form, which depends on the concentration of defects, is obtained at different crystallization temperatures. The values of the maximum amount of  $\gamma$  form ( $f_{\gamma}(\max)$ ), evaluated from the maximum of the curves of Figure 2, are reported in Figure 3 as a function of hexene concentration (Figure 3A) and of the total concentration of defects  $\epsilon$  = [ $rr$ ] + [2,1e] + [hexene] (Figure 3B), compared with the values of  $f_{\gamma}(\max)$  obtained in the literature for propylene–ethylene (iPPet) and propylene–butene (iPPBu) copolymers prepared with the same catalyst **A**.<sup>6</sup>

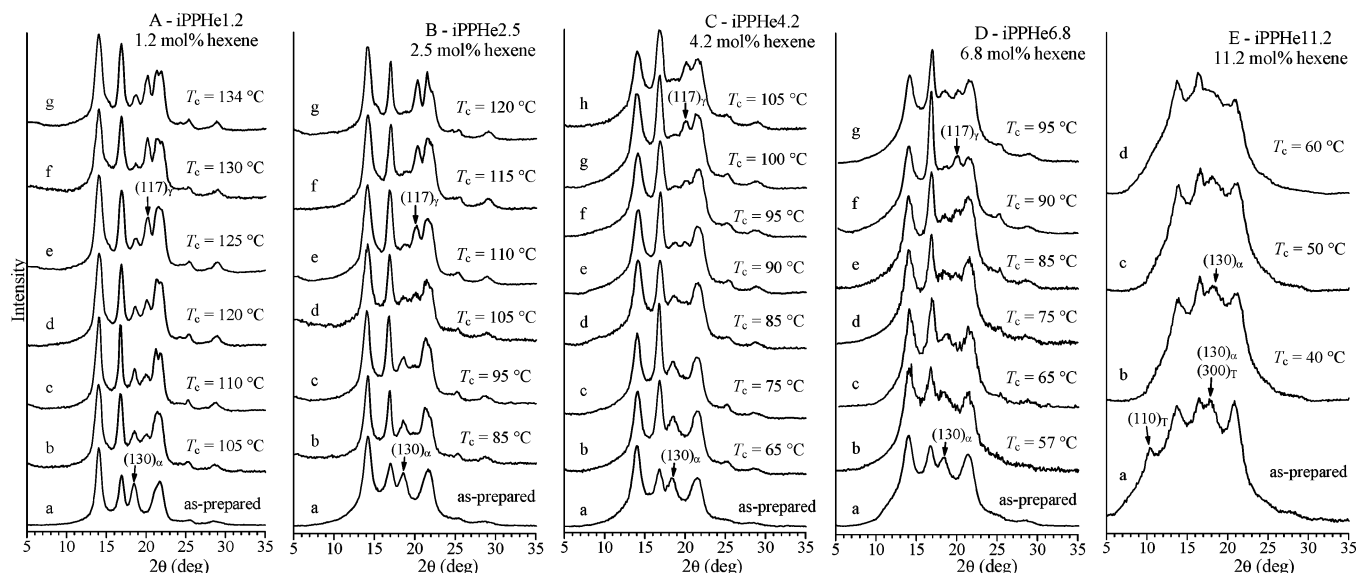


**Figure 1.** X-ray powder diffraction profiles of some samples of iPPHe copolymers isothermally crystallized from the melt at the indicated crystallization temperature  $T_c$ . The  $(130)_\alpha$  reflection of the  $\alpha$  form at  $2\theta \approx 18.6^\circ$  and the  $(117)_\gamma$  reflection of the  $\gamma$  form at  $2\theta \approx 20^\circ$  are indicated. In (E) the  $(110)_\gamma$  and  $(300)_\gamma$  reflections at  $2\theta = 10^\circ$  and  $17^\circ$  of the trigonal form are also indicated. The diffraction profiles of samples as-prepared and aged at room temperature (profiles a) are reported for comparison.

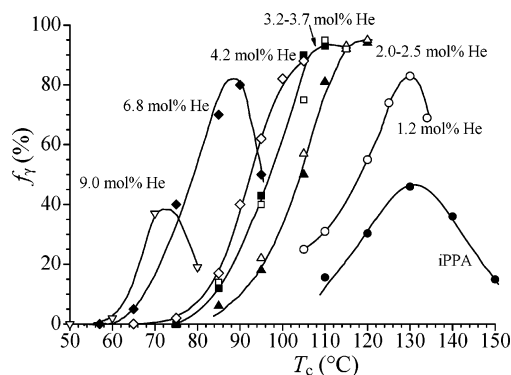


**Figure 2.** Relative amount of  $\gamma$  form of iPP,  $f_\gamma$ , evaluated from the X-ray diffraction profiles of Figure 1, in samples of iPPHe copolymers prepared with the catalyst A, isothermally crystallized from the melt, as a function of the crystallization temperature  $T_c$ : (●) sample iPPA; (○) sample iPPHe1.2; (△) sample iPPHe2.0; (▲) sample iPPHe2.5; (□) sample iPPHe3.2; (■) sample iPPHe3.7; (◇) sample iPPHe4.2; (◆) sample iPPHe6.8; (▽) sample iPPHe9.0. The concentrations (mol %) of hexene units (He) are indicated.

It is apparent that for iPPHe copolymers  $f_\gamma(\text{max})$  first increases, rapidly achieves a nearly constant maximum value of  $f_\gamma \approx 100\%$  already for hexene content of 2–3 mol %, and then decreases with increasing hexene content (Figure 3).

This behavior is similar to that of iPPBu copolymers but different from that of iPPet copolymers for which the value of  $f_\gamma(\text{max})$  increases with increasing ethylene concentration up to achieve the maximum value  $f_\gamma(\text{max}) = 100\%$  that remain constant for all ethylene concentrations compatible with the crystallization (Figure 3B).<sup>6</sup> Moreover, the increase of  $f_\gamma(\text{max})$  for iPPHe copolymers is much faster than for iPPBu copolymers, so that at low comonomer concentration in the range 2–3 mol % iPPHe copolymers produce maximum amount of  $\gamma$  form higher than that of iPPBu copolymers and even higher than that of iPPet samples (Figure 3B). Furthermore, for iPPHe copolymers also the decrease of  $f_\gamma(\text{max})$  at higher comonomer concentration is faster than for iPPBu copolymers and starts at comonomer concentration lower than for iPPBu samples (4–5 mol % for iPPHe against 14–15 mol % for iPPBu, Figure 3B).

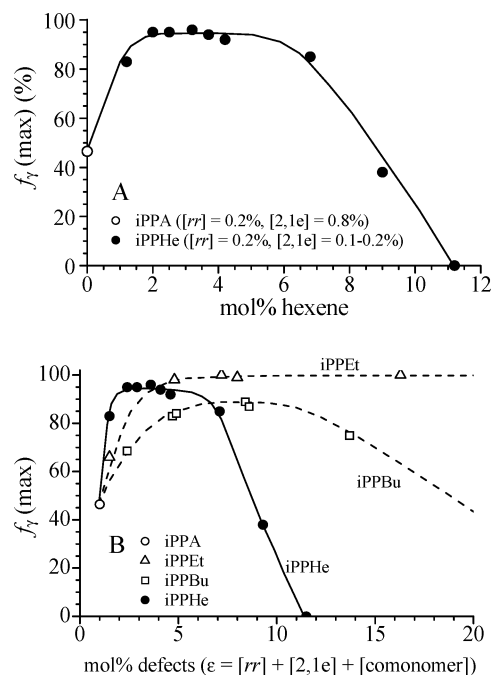


**Figure 3.** Maximum amount of  $\gamma$  form ( $f_\gamma(\text{max})$ ) obtained in iPPHe copolymers crystallized from the melt as a function of concentration of hexene units (A) and of total concentration of defects ( $\epsilon = [rr] + [2,1e] + [\text{comonomer}]$ ) (B). Data of  $f_\gamma(\text{max})$  obtained in the ref 6 for the homopolymer sample iPPA (A,B) and for iPPet and iPPBu copolymers (B) prepared with the same catalyst A are also reported for comparison.

Finally, samples with hexene content higher than 10 mol % (and lower than 15–16 mol %) crystallize exclusively in the  $\alpha$  form, whereas iPPBu copolymers crystallize totally in the  $\alpha$  form only at butene concentrations higher than 30 mol %.<sup>6</sup> Since all copolymers of Figure 3B are synthesized with the same highly isoselective catalyst A, the macromolecular chains of iPPet, iPPBu, and iPPHe copolymers present similar and very small concentration of *stereo*- and *regio*-defects, the different behavior of Figure 3B may be only related to the different influence of ethylene, butene, and hexene on the crystallization of iPP.

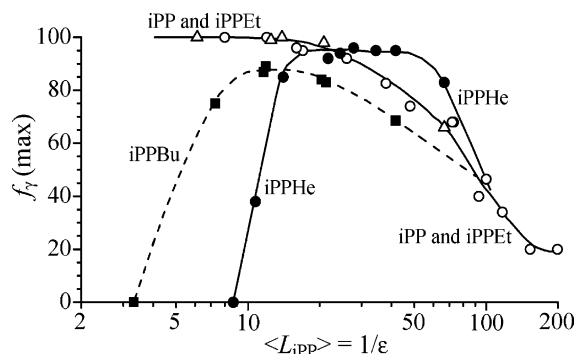


**Figure 4.** Maximum amount of  $\gamma$  form,  $f_{\gamma}(\max)$ , crystallized by isothermal crystallizations from the melt, evaluated from the maxima of the curves of Figure 2, as a function of the average length of fully isotactic propylene sequences  $\langle L_{iPP} \rangle$ , for samples of iPPHe copolymers prepared with the catalyst A (●) compared with data obtained for iPPBu (■) and iPPeT (△) copolymers in ref 6 and for samples of iPP homopolymer of different stereoregularity (including the sample iPPA), characterized by the presence of variable amount of  $rr$  stereodeficts, taken from refs 14 and 15a (○). The average length of fully isotactic propylene sequences has been evaluated as  $\langle L_{iPP} \rangle = 1/\epsilon$ , where  $\epsilon$  is the total concentration of defects  $\epsilon = [rr] + [2,1e] + [\text{comonomer}]$ . In the case of stereodeficient homopolymer samples the values of  $\langle L_{iPP} \rangle$  have been evaluated from the  $^{13}\text{C}$  NMR data,<sup>14</sup> as  $\langle L_{iPP} \rangle = (2[mm]/[mr]) + 2$ .

These data are consistent with recent results of studies on iPPeT and iPPBu copolymers prepared with various metallocene catalysts<sup>6</sup> that have shown that the role of defects on the crystallization of iPP is not only limited to the effect of shortening the length of regular fully isotactic sequences but also related to their possible inclusion into crystals of  $\alpha$  and  $\gamma$  forms. The crystallization of  $\gamma$  form is, indeed, believed to be favored when the regular isotactic sequences are short,<sup>6,12–21</sup> and, therefore, when the total concentration of any type of defects is high. However, differences in the degree of inclusion of different comonomers in the crystals of iPP leads to contents of the  $\gamma$  phase that differ among the copolymers.<sup>6,19,20</sup> According to a widely accepted view, butene enters to high extents in the iPP crystalline lattice, while ethylene, hexene, and octene enter to very limited degrees, causing substantial crystallinity reduction.<sup>19b,20</sup> The more excluded the comonomer unit is from the crystalline lattice, the higher would be the concentration of the  $\gamma$  form.<sup>19b</sup>

For iPPHe copolymers it has been demonstrated that hexene units are included in the crystals of iPP.<sup>2</sup> The accepted hypothesis that the amount of incorporated hexene units is much lower than those of butene and ethylene in the crystals of the corresponding copolymers is consistent with the data of Figure 3B that the amount of crystallized  $\gamma$  form of iPPHe copolymers at low hexene concentration, up to 2–3 mol %, is higher than that observed in iPPeT and iPPBu copolymers, but is not consistent with the fast decrease of the concentration of  $\gamma$  form with further increasing hexene concentration (Figure 3B).

A relationship between the maximum amount of  $\gamma$  form  $f_{\gamma}(\max)$  and the average length of regular propylene sequences  $\langle L_{iPP} \rangle$  has been recently found for stereodeficient iPP homopolymer samples, containing one type of defects ( $rr$  triads) in a wide range of concentration and free from any other microstructural defects.<sup>14</sup> The values of maximum amount of  $\gamma$  form  $f_{\gamma}(\max)$  obtained for iPPHe copolymers (Figure 3) are reported in Figure 4 as a function of the average length of the regular polypropylene sequences  $\langle L_{iPP} \rangle$  and compared with the relationship found for iPP homopolymer samples<sup>14</sup> and for iPPeT and iPPBu copolymers taken from ref 6. For copolymer samples, containing  $rr$  stereodeficts, 2,1 regiodefects, and comonomers,

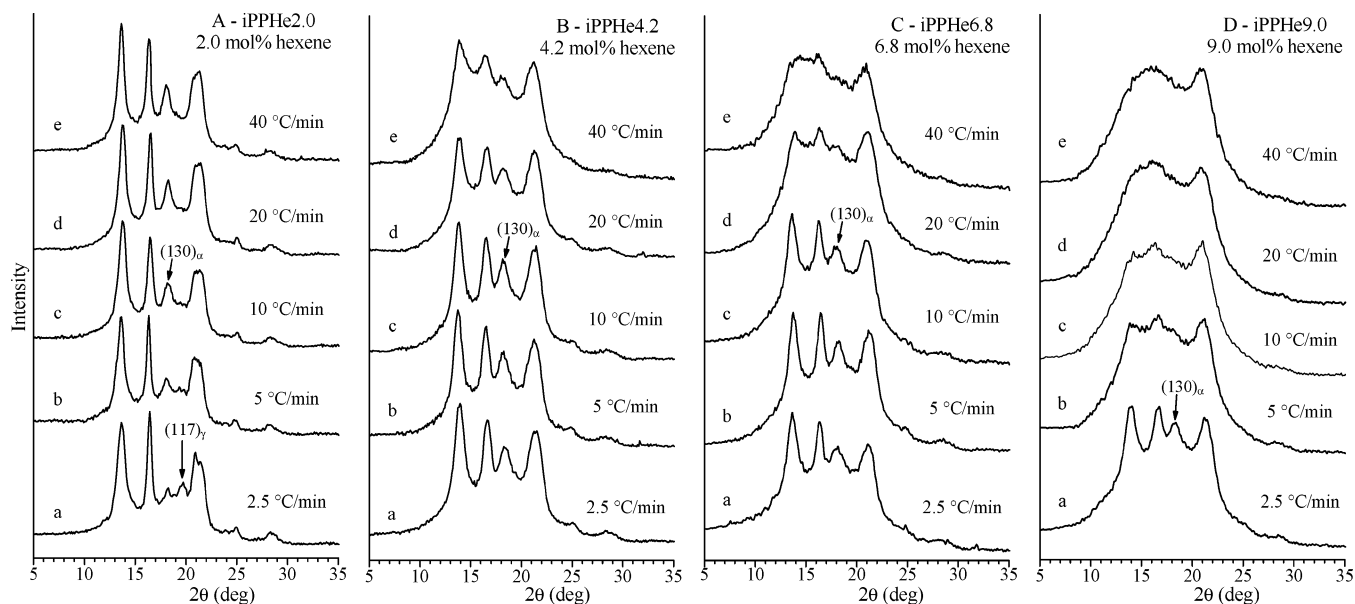
the average length of regular isotactic polypropylene sequences can be roughly evaluated as  $\langle L_{iPP} \rangle = 1/\epsilon$ , where  $\epsilon = [rr] + [2,1e] + [\text{comonomer}]$  is the total concentration of defects (Table 1).

Figure 4 clearly indicates that the data of iPPHe copolymers give a relationship between  $f_{\gamma}(\max)$  and  $\langle L_{iPP} \rangle$  different from those found for iPPeT and iPPBu copolymers<sup>6</sup> and for stereo-deficient iPP samples.<sup>14,15a</sup> As shown in ref 6, the data of  $f_{\gamma}(\max)$  obtained for iPPeT copolymers are well-interpolated by the same curve corresponding to the data of the stereoirregular iPP samples. Samples of iPP homopolymers containing only  $rr$  defects and iPPeT copolymers characterized by the same value of  $\langle L_{iPP} \rangle$  give the same maximum amount of  $\gamma$  form, regardless of the relative concentrations of  $rr$  and ethylene units. Therefore, ethylene comonomeric units and  $rr$  stereodeficts exert a similar effect on the crystallization of iPP, producing a similar effect of shortening the regular fully isotactic propylene sequences and inducing crystallization of  $\gamma$  form. At high defect concentration ( $\epsilon$  higher than 5–7 mol %) and low average length of iPP sequences ( $\langle L_{iPP} \rangle$  lower than 15–20 monomeric units) crystallization of the pure  $\gamma$  form is observed in both iPP homopolymer<sup>14</sup> and iPPeT copolymer samples.<sup>6</sup>

The data of  $f_{\gamma}(\max)$  for samples of iPPHe and iPPBu copolymers are, instead, not fitted by the master curve corresponding to the data of the stereoirregular iPP homopolymer and iPPeT copolymer samples (Figure 4), and different relationships between  $f_{\gamma}(\max)$  and  $\langle L_{iPP} \rangle$  are obtained depending on the comonomer. Moreover, iPPBu copolymers always produce values of maximum amount of  $\gamma$  form lower than those obtained for stereodeficient iPP homopolymers, iPPeT and iPPHe copolymers having the same value of  $\langle L_{iPP} \rangle$ ,<sup>6</sup> at least for  $\langle L_{iPP} \rangle$  higher than 20 monomeric units. Samples of iPPHe copolymers show instead a peculiar behavior because they produce the highest values of maximum amount of  $\gamma$  form for low hexene concentration and high values of  $\langle L_{iPP} \rangle$ , even higher than those obtained for stereodeficient iPP homopolymers and iPPeT copolymers, and the lowest values of maximum amount of  $\gamma$  form already for values of  $\langle L_{iPP} \rangle$  lower than 15–20 monomeric units and hexene concentration higher than 3–4 mol % (Figure 4). It is, indeed, sufficient that the hexene concentration achieves values not particularly high (around 4 mol %) to observe a fast decrease of the amount of  $\gamma$  form (Figures 3 and 4) and samples with hexene contents higher than 10 mol % (and lower than 15–16 mol %) crystallize exclusively in the  $\alpha$  form ( $f_{\gamma}(\max) = 0$ ). Surprisingly, as in the case of iPPBu copolymers, we find that for iPPHe copolymers the crystallization of  $\alpha$  form is favored for low values of the average length of the regular propylene sequences  $\langle L_{iPP} \rangle$ .

These data confirm the idea that the crystallization of  $\gamma$  form of iPP is related not only to the value of the average length of the regular fully isotactic propylene sequences  $\langle L_{iPP} \rangle$  but also to the inclusion of defects in the crystals and the different compatibility of the different defects within the crystalline lattices of  $\alpha$  and  $\gamma$  forms of iPP, which produces differences in the partitioning of defects between crystals of  $\alpha$  and  $\gamma$  forms.<sup>6</sup>

According to a more general view, the crystallization properties and polymorphic behavior of iPP and corresponding copolymers depend on a double role played by stereodeficts, regiodefects, and constitutional defects. The first effect is the interruption of the regular fully isotactic propylene sequences with shortening of the average length of the crystallizable sequences  $\langle L_{iPP} \rangle$ , which favors crystallization of  $\gamma$  form. This effect is common to any defects (*stereo*- and *regio*-defects and comonomeric units) and may be more or less efficient depending



**Figure 5.** X-ray powder diffraction profiles of some samples of iPPHe copolymers crystallized from the melt by cooling the melt at the indicated cooling rates. The  $(130)_\alpha$  reflection of the  $\alpha$  form at  $2\theta \approx 18.6^\circ$  and the  $(117)_\gamma$  reflection of the  $\gamma$  form at  $2\theta \approx 20^\circ$  are indicated.

on the effective disturbance of the defect, which, in turn, is related, in the case of copolymers, to the size of the comonomeric units. The second effect is due to the possible inclusion of defects in the crystals of  $\alpha$  and  $\gamma$  forms of iPP. This favors crystallization of the crystalline form that better tolerates the defect within its crystalline lattice.

As discussed above, butene enters to high extents in the iPP lattice, while ethylene and hexene enter to limited degrees.<sup>19b,20</sup> However, in the case of hexene this is true only at low concentrations. It has been, indeed, recently demonstrated that the degree of inclusion of hexene units into crystals of iPP is different depending on the composition.<sup>2</sup> In iPPHe copolymers with low hexene concentration, up to 3–4 mol %, hexene units are only partially included into crystals acting as a real defect,<sup>1,2</sup> whereas in samples with higher hexene concentration a higher amount of hexene units tends to enter into crystals of  $\alpha$  form, acting as structural features, because this produces an increase of crystalline density, which, in turn, induces crystallization of the trigonal form of iPP.<sup>1,2</sup> The density-driven crystallization of the trigonal form, therefore, forces hexene units to enter to high extents even in the crystals of  $\alpha$  form at hexene concentration in the range 4–11 mol %, before the crystallization of the trigonal form.

Therefore, for iPPHe copolymers with low hexene concentration (up to 2–3 mol %), hexene units are included to limited degrees in the crystals of  $\alpha$  and  $\gamma$  form; hence, the effect of interruption of the regular fully isotactic propylene sequences, with shortening the average length of the crystallizable sequences  $\langle L_{iPP} \rangle$ , prevails and induces crystallization of  $\gamma$  form. This effect of interruption of hexene units is more efficient than that of *rr* defects or ethylene and butene units because of the bigger size and greater disturbance of hexene units and explains the fast increase of the maximum amount of  $\gamma$  form for iPPHe copolymers with increasing hexene content (Figure 3) and decreasing  $\langle L_{iPP} \rangle$  in the range 150–50 monomeric units (Figure 4) and the higher amount of  $\gamma$  form that crystallize in iPPHe copolymers at low comonomer concentrations with respect to stereodeficient iPP homopolymers and iPP*Et* and iPP*Bu* copolymers (Figure 4). For hexene contents higher than 3–4 mol %, the effect of inclusion of hexene units into crystals of  $\alpha$  form, driven by the density increase, prevails over that of the

shortening of  $\langle L_{iPP} \rangle$  and induces crystallization of  $\alpha$  form. This explains the fast decrease of the amount of  $\gamma$  form observed for  $\langle L_{iPP} \rangle$  lower than 15–20 monomeric units (Figure 4) and the crystallization of iPPHe copolymers with hexene content higher than 10 mol % (and lower than 15–16 mol %) in the pure  $\alpha$  form.

The crystallization of the iPPHe copolymers has also been studied in nonisothermal conditions to compare the thermodynamic and kinetic factors that drive the crystallization of  $\alpha$  and  $\gamma$  forms. The X-ray diffraction profiles of some samples of iPPHe copolymers crystallized by cooling the melt at cooling rates of 40, 20, 10, 5, and 2.5 °C/min are reported in Figure 5 as examples.

The absence of the  $(117)_\gamma$  reflection of the  $\gamma$  form in all profiles of Figure 5 clearly indicates that all samples tend to crystallize by cooling the melt in the  $\alpha$  form at any cooling rate. Only in the case of samples with low hexene concentrations and only at the lowest cooling rate, a low amount of  $\gamma$  form crystallize from the melt (for instance the sample iPPHe2.0 with 2.0 mol % of hexene at cooling rate of 2.5 °C/min, profile a of Figure 5A). At higher hexene concentration and high cooling rates a strong decrease of crystallinity is observed (Figure 5C,D) and samples with hexene content higher than 9 mol % do not crystallize, and amorphous samples are obtained by cooling the melt to room temperature.<sup>2</sup>

The comparison between the data of Figure 5 and those of the isothermal melt-crystallizations of Figures 1–3 indicates that in iPPHe copolymers, as in stereodeficient iPPs homopolymers,<sup>13,15b</sup> the  $\alpha$  form is always kinetically favored because it forms at high crystallization rates, as by fast cooling the melt (Figure 5). The formation of  $\gamma$  form is instead thermodynamically favored because it crystallizes in the slow isothermal crystallizations, but only for hexene concentrations lower than 3–4 mol %, for which the effect of interruption of the regular propylene sequences prevails. At hexene concentrations higher than 6–7 mol %, the  $\alpha$  form turns out to be also thermodynamically, besides than kinetically, favored because it preferentially crystallizes in both slow isothermal (Figures 1–3) and fast nonisothermal crystallizations. At these hexene contents, indeed, the effect of inclusion of hexene units in the crystals of

$\alpha$  form, driven by density increase, prevails over that of interruption of the propylene sequences.

### Concluding Remarks

Samples of iPPHe copolymers crystallize from the melt as mixtures of  $\alpha$  and  $\gamma$  forms; the relative fraction of  $\gamma$  form increases with increasing crystallization temperature. The maximum amount of  $\gamma$  form first increases very rapidly with increasing hexene concentration, up to 2–3 mol %, and then rapidly decreases for hexene concentrations higher than 4–5 mol %, and samples with hexene contents higher than 10 mol % crystallize from the melt exclusively in the  $\alpha$  form. For concentrations higher than 15–16 mol % iPPHe copolymers do not crystallize from the melt, but amorphous samples crystallize into the trigonal form at room temperature.<sup>1,2</sup>

These data and the comparison with the amount of  $\gamma$  form crystallized from the melt in stereodeficient iPP homopolymer samples and iPPet and iPPBu copolymers reported in the literature<sup>6,14</sup> have confirmed that the crystallization of  $\gamma$  form of iPP is not only related to the value of the average length of the regular fully isotactic propylene sequences  $\langle L_{iPP} \rangle$ , which in turn depends on the total concentration of defects, but also related to the different degrees of inclusion of stereodeficient and constitutional defects in the crystals of  $\alpha$  and  $\gamma$  forms of iPP.

Stereodeficient, regiodeficient, and constitutional defects play a double role. The first effect that favors crystallization of  $\gamma$  form is the interruption of the regular isotactic propylene sequences with shortening the average length of the regular isotactic sequences  $\langle L_{iPP} \rangle$ . The second effect is due to the possible inclusion of defects in the crystals of the polymorphic forms of iPP that favors crystallization of  $\alpha$  or  $\gamma$  forms depending on which of the two forms better tolerate the defect within its crystalline lattice. Depending on which effect is prevalent, *rr* stereodeficient and ethylene, butene, and hexene comonomeric units exert different influences on the crystallization of  $\alpha$  and  $\gamma$  forms of iPP.

Ethylene comonomeric units and *rr* stereodeficient are included in crystals of both  $\alpha$  and  $\gamma$  forms, but probably, they are more easily included in crystals of  $\gamma$  form and in  $\alpha/\gamma$  disordered modifications of  $\gamma$  form and, hence, favor crystallization of  $\gamma$  form. Therefore, in iPPet copolymers and in stereodeficient iPP homopolymers the two effects of crystal inclusion and of shortening the regular fully isotactic propylene sequences are added and produce the same result of favoring the crystallization of  $\gamma$  form.<sup>6</sup> This results in a similar polymorphic behavior of stereodeficient iPPs and iPPet copolymers (Figure 4). In the case of iPPBu copolymers, butene units are included indifferently in crystals of  $\alpha$  and  $\gamma$  forms, but probably more easily in the  $\alpha$  form at high concentrations. Therefore, at low butene concentration, up to nearly 10 mol %, the effect of shortening the length of regular isotactic propylene sequences prevails and induces crystallization of  $\gamma$  form, whereas for butene concentrations higher than 10 mol % the effect of inclusion of butene units in crystals of  $\alpha$  form and the complete compatibility of propylene and butene units in crystals of  $\alpha$  form prevails over that of the shortening of  $\langle L_{iPP} \rangle$  and induces crystallization of  $\alpha$  form.<sup>6</sup> Hexene units are instead preferably included in crystals of  $\alpha$  form driven by the density increase and, therefore, favor crystallization of  $\alpha$  form at high concentrations (lower than 15–16 mol %). At low hexene concentrations the degree of inclusion

in the crystals is low and the effect of shortening of  $\langle L_{iPP} \rangle$  is very efficient, because of the bigger size of hexene units, and prevails over that due to the crystal inclusion. This induces crystallization of the highest concentration of  $\gamma$  form. This view explains the results that iPPHe copolymers develop by melt-crystallization amounts of  $\gamma$  form higher or much lower than those obtained in iPPet and iPPBu copolymers and in stereodeficient iPPs,<sup>6,14</sup> at low (up to 2–3 mol %) or high (higher than 4–5 mol %) hexene concentration, respectively.

**Acknowledgment.** Financial support from Basell Polyolefins, Ferrara (Italy) is gratefully acknowledged.

### References and Notes

- (1) De Rosa, C.; Auriemma, F.; Corradini, P.; Tarallo, O.; Dello Iacono, S.; Ciaccia, E.; Resconi, L. *J. Am. Chem. Soc.* **2006**, *128*, 80.
- (2) De Rosa, C.; Dello Iacono, S.; Auriemma, F.; Ciaccia, E.; Resconi, L. *Macromolecules* **2006**, *39*, 6098.
- (3) Poon, B.; Rogunova, M.; Hiltner, A.; Baer, E.; Chum, S. P.; Galeski, A.; Piorkowska, E. *Macromolecules* **2005**, *38*, 1232.
- (4) Lotz, B.; Ruan, J.; Thierry, A.; Alfonso, G. C.; Hiltner, A.; Baer, E.; Piorkowska, E.; Galeski, A. *Macromolecules* **2006**, *39*, 5777.
- (5) Natta, G.; Corradini, P.; Bassi, I. W. *Nuovo Cimento, Suppl.* **1960**, *15*, 52.
- (6) De Rosa, C.; Auriemma, F.; Ruiz de Ballesteros, O.; Resconi, L.; Camurati, I. *Macromolecules* **2007**, *40*, 6600.
- (7) Bingel, C.; Goeres, M.; Fraaije, V.; Winter, A. (Targor) Int. Pat. Appl. WO 1998/040331.
- (8) Resconi, L.; Ciaccia, E.; Fait, A. (Basell: Italy) Int. Pat. Appl. WO 2004/092230.
- (9) (a) Ewen, J. A.; Elder, M. J.; Jones, R. L.; Rheingold, A. L.; Liable-Sands, L. M.; Sommer, R. D. *J. Am. Chem. Soc.* **2001**, *123*, 4763. (b) Int. Pat. Appl. WO 44318 (2001), Basell, invs.: Ewen, J. A.; Elder, M. J.; Jones, R. L.
- (10) (a) Forlini, F.; Tritto, I.; Locatelli, P.; Sacchi, M. C.; Piemontesi, F. *Macromol. Chem. Phys.* **2000**, *201*, 401. (b) Kissin, Y. V.; Brandolini, A. *J. Macromolecules* **1991**, *24*, 2632. (c) Zhang, Y. *Polymer* **2004**, *45*, 2651.
- (11) Kakugo, M.; Naito, Y.; Mizunuma, K.; Miyatake, T. *Macromolecules* **1982**, *15*, 1150.
- (12) De Rosa, C.; Auriemma, F.; Circelli, T.; Waymouth, R. M. *Macromolecules* **2002**, *35*, 3622.
- (13) Auriemma, F.; De Rosa, C. *Macromolecules* **2002**, *35*, 9057.
- (14) De Rosa, C.; Auriemma, F.; Di, Capua, A.; Resconi, L.; Guidotti, S.; Camurati, I.; Nifant'ev, I. E.; Laishchev, I. P. *J. Am. Chem. Soc.* **2004**, *126*, 17040.
- (15) (a) De Rosa, C.; Auriemma, F.; Paolillo, M.; Resconi, L.; Camurati, I. *Macromolecules* **2005**, *38*, 9143. (b) De Rosa, C.; Auriemma, F.; Resconi, L. *Macromolecules* **2005**, *38*, 10080.
- (16) (a) Fischer, D.; Mülhaupt, R. *Macromol. Chem. Phys.* **1994**, *195*, 1433. (b) Thomann, R.; Wang, C.; Kressler, J.; Mülhaupt, R. *Macromolecules* **1996**, *29*, 8425. (c) Thomann, R.; Semke, H.; Maier, R. D.; Thomann, Y.; Scherble, J.; Mülhaupt, R.; Kressler, J. *Polymer* **2001**, *42*, 4597.
- (17) (a) Alamo, R. G.; Kim, M. H.; Galante, M. J.; Isasi, J. R.; Mandelkern, L. *Macromolecules* **1999**, *32*, 4050. (b) VanderHart, D. L.; Alamo, R. G.; Nyden, M. R.; Kim, M. H.; Mandelkern, L. *Macromolecules* **2000**, *33*, 6078.
- (18) (a) Arnold, M.; Henschke, O.; Knorr, J. *Macromol. Chem. Phys.* **1996**, *197*, 563. (b) Arnold, M.; Bornemann, S.; Köller, F.; Menke, T. J.; Kressler, J. *Macromol. Chem. Phys.* **1998**, *199*, 2647. (c) Busse, K.; Kressler, J.; Maier, R. D.; Scherble, J. *Macromolecules* **2000**, *33*, 8775.
- (19) (a) Alamo, R. G.; VanderHart, D. L.; Nyden, M. R.; Mandelkern, L. *Macromolecules* **2000**, *33*, 6094. (b) Hosier, I. L.; Alamo, R. G.; Estes, P.; Isasi, G. R.; Mandelkern, L. *Macromolecules* **2003**, *36*, 5623. (c) Hosier, I. L.; Alamo, R. G.; Lin, J. S. *Polymer* **2004**, *45*, 3441. (d) Alamo, R. G.; Ghosal, A.; Chatterjee, J.; Thompson, K. L. *Polymer* **2005**, *46*, 8774.
- (20) Hosoda, S.; Hori, H.; Yada, K.; Tsuji, M.; Nakahara, S. *Polymer* **2002**, *43*, 7451.
- (21) Stagnaro, P.; Costa, G.; Trefiletti, V.; Canetti, M.; Forlini, F.; Alfonso, G. C. *Macromol. Chem. Phys.* **2006**, *207*, 2128.

MA071753+